ELSEVIER

# Modeling of the power cable production line

Vanja Kosar *, Zoran Gomzi

*Faculty of Chemical Engineering and Technology, Department of Reaction Engineering and Catalysis,
University of Zagreb, Savska c. 16, HR-10000 Zagreb, Croatia*

## Abstract

During the manufacturing of a power cable insulated with the cross-linkable polyethylene, the hot polymer is applied to the conductor by extrusion, below temperatures of the rapid cross-linking. The coated cable passes into a high-pressure tube (filled with nitrogen under the pressure of 10 bar) in order to heat up the insulation to temperatures at which the cross-linking agent is highly active. This is the continuous vulcanization (CV) tube. Changes of process variables associated with the CV tube can cause changes in the physical properties, the aging characteristics, and especially the heat resistance of the cable insulation. Performance of insulating compounds in this area of the cross-linking process can determine maximum output rates of a power cable manufacturing facility.

The mathematical model describes cross-linking process in the vulcanization tube, which is in fact a tubular reactor. In the vulcanization tube heat is transferred by convection, conduction and radiation. Also, the reaction heat is liberated by the chemical reaction and the heat balance describes all four impacts. Formal part of the mathematical model is a material balance that describes the reactions kinetics. Heat and mole balance are connected with reaction rate and mathematically present a system of partial differential equations which will be numerically solved for chosen boundary conditions, both for the reaction part and for the cooling part of a process. On the basis of the real process parameters and the presented mathematical model simulation of the process was conducted.

From the presented simulation the optimal process parameters such as process temperatures, cable linear velocity ($u$) and cable cooling properties of CV line are predicted and evaluated.
© 2007 Elsevier B.V. All rights reserved.

*Keywords:* Vulcanization; Cross-linking; Vulcanization tube; XLPE 4201; Dicumyl peroxide; Medium voltage power cable; Mathematical model; Simulation

## 1. Introduction

Development and progress of the cable production technology demand a reliable mathematical model which would serve as a basis for simulation and optimization of the vulcanization process as a whole. Because of a complexity of the vulcanization process which includes chemical reactions inside the polymer insulation, a heat transfer during the reaction (heating) as well as a cooling period inside the cable and vulcanization tube, there is a need to solve separately individual parts which would be at the end joined together in the model. The obtained model can be used as a starting point in the computer programs that aim to find optimal values of the process parameters.

The purpose of this study (i.e. the modeling) is to propose a mathematical model of the dry cured vulcanization of the XLPE

insulation material as well as to validate it on the data obtained in the actual process (i.e. the production line).

### 1.1. Cross-linking reaction

The most widely used technique for the insulation material curing is a cross-linking of polyethylene (PE) with organic peroxides. These peroxides (e.g. dicumyl peroxide, DCP) decompose at the elevated temperatures to generate free radicals [1,2]. These radicals abstract hydrogen atoms from the polymer chains to form reactive sites. Two reactive sites in different chains can recombine and form a chemical bond and the reaction leads to a network structure [3]. The chemical process of PE cross-linking by DCP in the presence of antioxidant is illustrated in Fig. 1.

This network combines good electrical properties with an improved heat deformation characteristic in comparison with the standard LDPE required for the MV/HV insulated cables [4–7].

* Corresponding author. Tel.: +385 1 4597146; fax: +385 1 4597133.
   *E-mail address:* vkosar@marie.fkit.hr (V. Kosar).

## Nomenclature

| | |
|---|---|
| $A_r$ | Arrhenius number (min$^{-1}$) |
| $A_1, A_2$ | area of heat exchange (m$^2$) |
| $c_i$ | initiator concentration (mol m$^{-3}$) |
| $c_{pj}$ | conductor specific heat capacity (kJ kg$^{-1}$ K$^{-1}$) |
| $c_{pp}$ | insulation specific heat capacity (kJ kg$^{-1}$ K$^{-1}$) |
| $c_{pH_2O}$ | water specific heat capacity (kJ kg$^{-1}$ K$^{-1}$) |
| $d$ | core diameter (m) |
| $E_a$ | activation energy (kJ mol$^{-1}$) |
| $Gr$ | Grashoff number |
| $h_{air}$ | air heat transfer coefficient (kJ s$^{-1}$ m$^{-2}$ K$^{-1}$) |
| $h_{H_2O}$ | water heat transfer coefficient (kJ s$^{-1}$ m$^{-2}$ K$^{-1}$) |
| $\Delta H_r$ | heat of reaction (kJ kg$^{-1}$) |
| $k_i$ | rate constant of initiator decomposition (s$^{-1}$) |
| $L$ | cable length (m) |
| $N$ | number of experimental points (Eq. (7)) |
| $Nu$ | Nusselt number |
| $n, m$ | kinetic constants |
| $P$ | theoretical degree of cross-linking |
| $Pr$ | Prandtl number |
| $q_{rad}$ | radiation heat flux (kJ s$^{-1}$ m$^{-2}$) |
| $r$ | space coordinate in radial direction (m) |
| $r_i$ | rate of initiator decomposition (mol m$^{-3}$ s$^{-1}$) |
| $r_p$ | rate of cross-linking (mol m$^{-3}$ s$^{-1}$) |
| $R$ | cable radius (m) |
| $Re$ | Reynolds number |
| $R_g$ | gas constant (8.134 J mol$^{-1}$ K$^{-1}$) |
| $t$ | time (min) |
| $T_{air}$ | air temperature (°C) |
| $T_j$ | conductor temperature (°C) |
| $T_N$ | nitrogen temperature (°C) |
| $T_p$ | insulation temperature (°C) |
| $T_w$ | tube wall temperature (°C) |
| $u$ | cable linear velocity (m min$^{-1}$) |
| $u_{H_2O}$ | water flow rate (m s$^{-1}$) |
| $x$ | dimensionless radius |
| $\bar{y}_{i_{exp.}}$ | normalized value of experimental dependent variable |
| $\bar{y}_{i_{theor.}}$ | normalized value of theoretical dependent variable |
| $z$ | space coordinate in axial direction (m) |

*Greek letters*

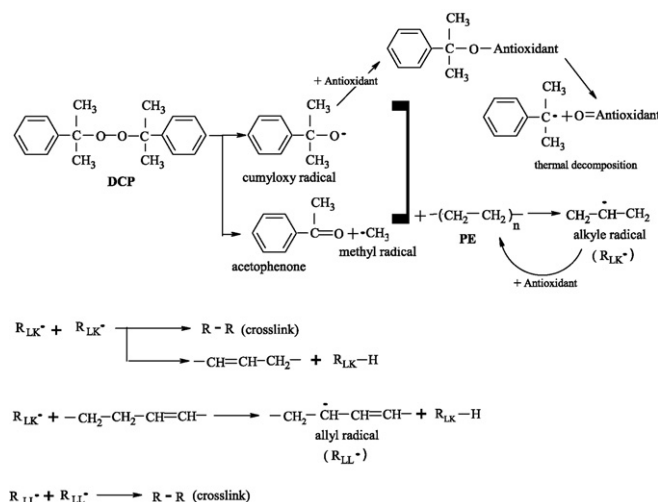| | |
|---|---|
| $\varepsilon$ | emissivity |
| $\lambda_j$ | conductor heat conductivity (kJ s$^{-1}$ m$^{-1}$ K$^{-1}$) |
| $\lambda_p$ | insulation heat conductivity (kJ s$^{-1}$ m$^{-1}$ K$^{-1}$) |
| $\lambda_N$ | nitrogen heat conductivity (kJ s$^{-1}$ m$^{-1}$ K$^{-1}$) |
| $\lambda_w$ | tube wall (iron) heat conductivity (kJ s$^{-1}$ m$^{-1}$ K$^{-1}$) |
| $\mu$ | dynamic viscosity (kg m$^{-1}$ s$^{-1}$) |
| $\rho_j$ | conductor density (Al) (kg m$^{-3}$) |
| $\rho_p$ | insulation density (Al) (kg m$^{-3}$) |
| $\rho_{H_2O}$ | water density (Al) (kg m$^{-3}$) |
| $\sigma$ | Stefan–Boltzmann constant (5.67 e$^{-8}$ W m$^{-2}$ K$^{-4}$) |



Fig. 1. Cross-linking reaction scheme for the polyethylene with the DCP and an antioxidant.

The cross-linking of polyethylene initiated with organic peroxide consists of a large number of chemical reactions, some of them leading to the linking of macromolecules, but some of the reactions have side effects (antioxidant may react with the alkyl radical of PE and decrease the alkyl and allyl radical concentrations) [8,9]. Since all of the reactions occur simultaneously, it is difficult to investigate kinetics of the particular reaction [10].

As a rate limited reaction the peroxide decomposition has a dominant part in the whole cross-linking mechanism. Its kinetics is of first order given by

$$r_i = k_i c_i \tag{1}$$

On this basis it is usual to describe the cross-linking reaction as *n*th order reaction with a degree of cross-linking, *P* as a variable [11]:

$$r_p = k(1 - P)^n \tag{2}$$

The rate constant, *k* is given by the Arrhenius equation:

$$k = A_r \exp\left(-\frac{E_a}{R_g T}\right) \tag{3}$$

### 1.2. Cable design

As shown in Fig. 2, a typical power cable is made of these elements [12]:

(1) *Conductor*. Copper or aluminium rope, compacted.
(2) *Conductor screen*. Semi-conductive layer over the conductor, carbon black is added as a conductive compound to the matrix of PE.
(3) *Insulation*. Cross-linked polyethylene—XLPE.
(4) *Insulation screen*. Semi-conductive layer over insulation—the same material used as in the conductor screen.
(5) *Separator I*. Swelling tape, absorbs water prior to their transition in the cable interior.
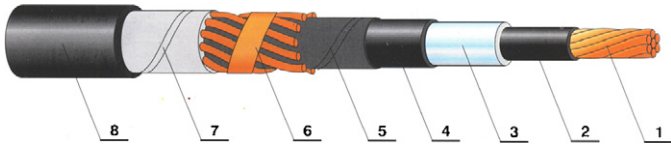(6) *Electric protection/screen*. Of copper wire.

Fig. 2. Construction of the medium voltage power cable.

(7) *Separator II*. Swelling tape.
(8) *External sheath*. Polyethylene, PE.

### 1.3. Cable production line

Medium voltage cables with XLPE insulation are manufactured using the recent technology of insulation in triple extrusion under simultaneous application of semi-conductive layers over conductor and insulation (triplex extrusion).

Cross-linking of polymer is done by dry curing under high pressure in a tube filled with nitrogen. As a result, high quality and tight connection between the insulation and the conductor is obtained without a possibility of their separation during the cable heating and cooling cycles [13]. Cross-linking in nitrogen atmosphere increases the resistance of insulation towards appearance and spreading of 'treeing' and thereby also of partial discharge. Better insulation properties considerably improve the grade of dielectric strength of insulation and prolong the lifetime of cables. Scheme of the production line is represented in Fig. 3.

In terms of product quality some requirements during the heating and curing cycles in the tube should be satisfied. First, at the end of the process the degree of cross-linking should be between 0.9 and 0.95 through the insulation layer. Also, the temperature at the end of the tube (after the water cooling) should be maximum 90 °C. Finally the temperature across the whole cable at the end of the process should not exceed 40 °C. These requirements are essential for the cable usage quality and should be monitored during the production process according to international standards for testing of the medium voltage cables [14].

Cross-linking reaction process depends on the polymer (insulation) type, concentration of an initiator and also on the process temperature. The main concern is a description of the temperature impact on the cross-linking reaction which is exothermic and may cause temperature gradients through the cable [15]. These temperature gradients can decrease the quality of the cable due to degradation of polymer chains. The cable must be heated at high temperature (around 170 °C), as a requirement for the cross-linking reaction.

During the continuous process in the curing tube the heat is transferred by radiation and convection from the tube wall through nitrogen to the cable surface [16]. At the same time heat is transferred through the cable (insulation and conductor) by conduction, Fig. 4a. Due to the exothermic cross-linking reaction inside the insulation some reaction heat, $\Delta H_r$, is released during the process.

After the heated part of the tube, the cable enters the water cooled part of the tube with the same velocity, $u_x$. In this part of the tube cable is cooled in water by force convection with a counter current flow of water between the cable and inner tube wall, Fig. 4b. Finally, after the cable exits the vulcanization tube, the cable is cooled by natural convection in the surrounding air, Fig. 4c.

Simultaneously with the cable cooling by convection, the heat is transferred inside the cable by conduction through the insulation and the core. Properly selected heating and cooling of the cable is the main experimental challenge to perform, control and optimize the process as a whole.

The plant for the continuous production of power cables is presented in Fig. 5. Process starts in an extruder (1) where the conductor (Cu or Al) is coated with the extruded polymer (insulation XLPE 4201). After that, the cable enters the heated part of the tube (2) filled with the high-pressured nitrogen under 10 bar where the cross-linking reaction occurred due to the heat transferred from the tube wall by radiation and convection. This part of the tube is separated in the six independent heat zones, and also before the water cooled part, there is one zone of the tube filled with nitrogen which is not heated. After that the cable is cooled to the ambient temperature in two steps. First, in the part of the tube cooled with cold water, also at pressure 10 bar (3) and finally after leaving the tube, the cable is cooled in the surrounding air by free convection (4) until the end of the process on the product wheel (5).
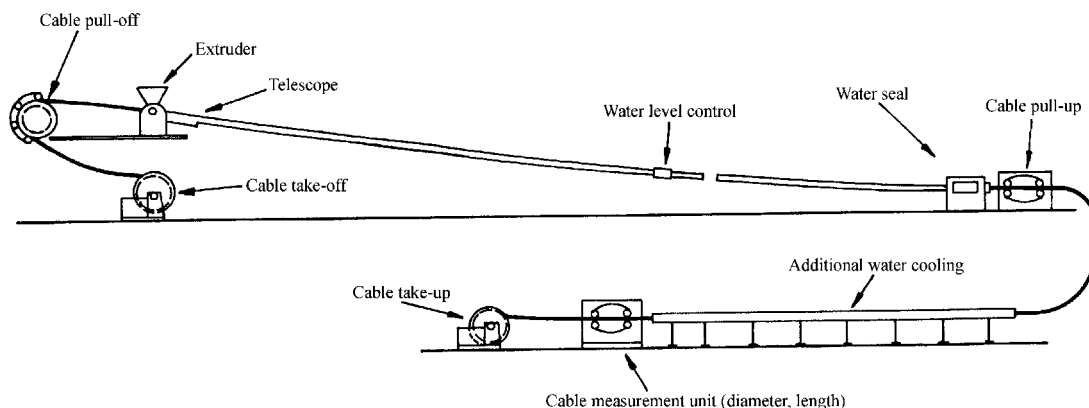


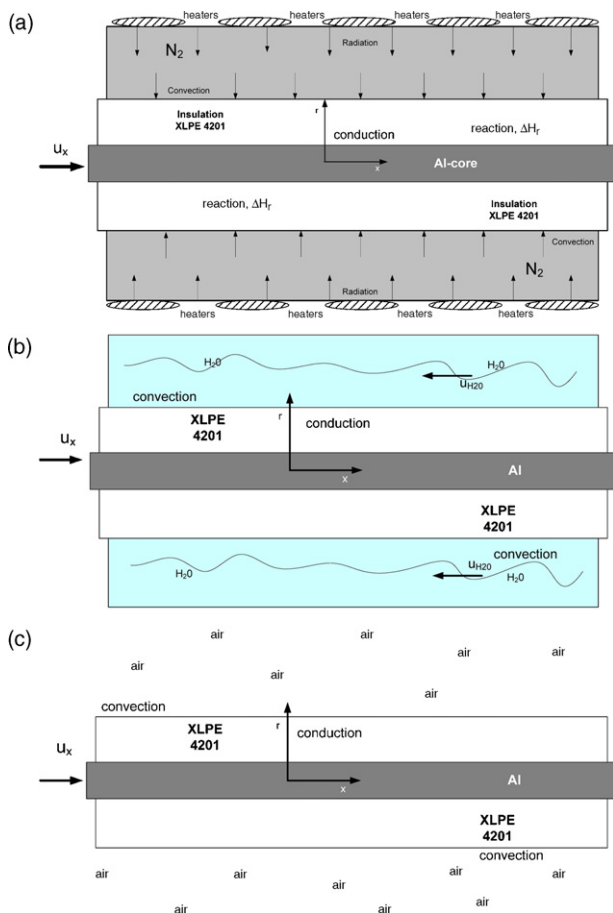Fig. 3. Schematic of the medium voltage cable production line.

Fig. 4. (a) Heat transfer in the heated (reaction) part of the vulcanization tube. (b) Heat transfer in the water cooled part of the vulcanization tube. (c) Heat transfer in the air cooled part of the process.

It is necessary for a properly conducted process that many parameters of the production line must be chosen carefully, namely: the line speed (governs the residence time in the tube), the temperature in the heated part of the tube filled with nitrogen, the temperature and flow rate of the cooling water. All of these requirements and restrictions are a part of the complex manufacturing of power cables and the manufactures select these values on their own.

## 2. Experimental

### 2.1. Materials

In this work used insulation material was a cross-linkable low density polyethylene, XLPE 4201 supplied by Borealis. This material has been used over last 20 years for insulation of medium and high voltage cables. Main advantages of cross-linking polyethylene over the standard LDPE are: good scorch resistance, good aging performance, resistance to water tree-ing, good insulation properties, low exudation of peroxide and antioxidance and cleanliness [17]. The dicumyl peroxide is an ingredient of PE premixture and its weight concentration is around 2%.

### 2.2. Analytical methods

To characterize properties of the cable as well as the used materials (insulation and conductor) many experiments have been performed. In this paper two of them will be presented: (1) determination of the cross-linking reaction kinetics by DSC, and (2) temperature measurements on the production line (surface of the vulcanization tube in the water cooled part and cable surface in the air cooled part of the process).

#### 2.2.1. DSC analysis

Calorimetric measurements were conducted in the Netzch thermal analyzer DSC 200 differential scanning calorimeter operating within the temperature range between −170 and 530 °C, equipped with a liquid nitrogen cooling system. Tests were performed both in isothermal and dynamic condition on the sample of 5–10 mg.

In this work only dynamic DSC scans will be analyzed. The reason for this is results inconsistence with the isothermal experiment due to a high temperature of the peroxide decomposition (over 160 °C, Fig. 6).

#### 2.2.2. Production line temperature measurements

To achieve some validation of the mathematical model temperatures were measured on the production line during the cable processing. Unfortunately, the heated part of the vulcanization
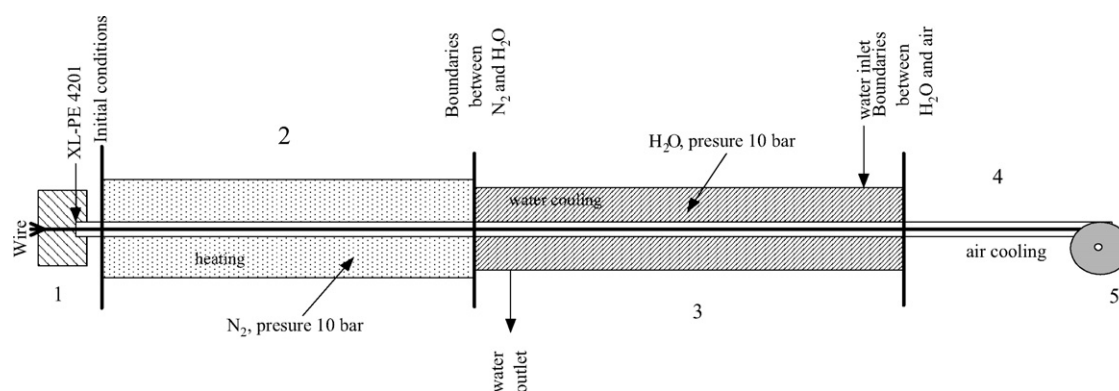


Fig. 5. Schematic of the continuous cross-linking and cable cooling process.
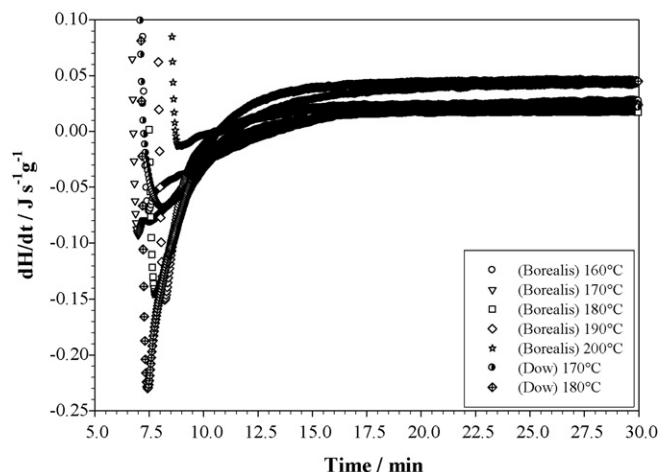
Fig. 6. Rate of heat evolved from the reaction as a function of time at different temperatures.
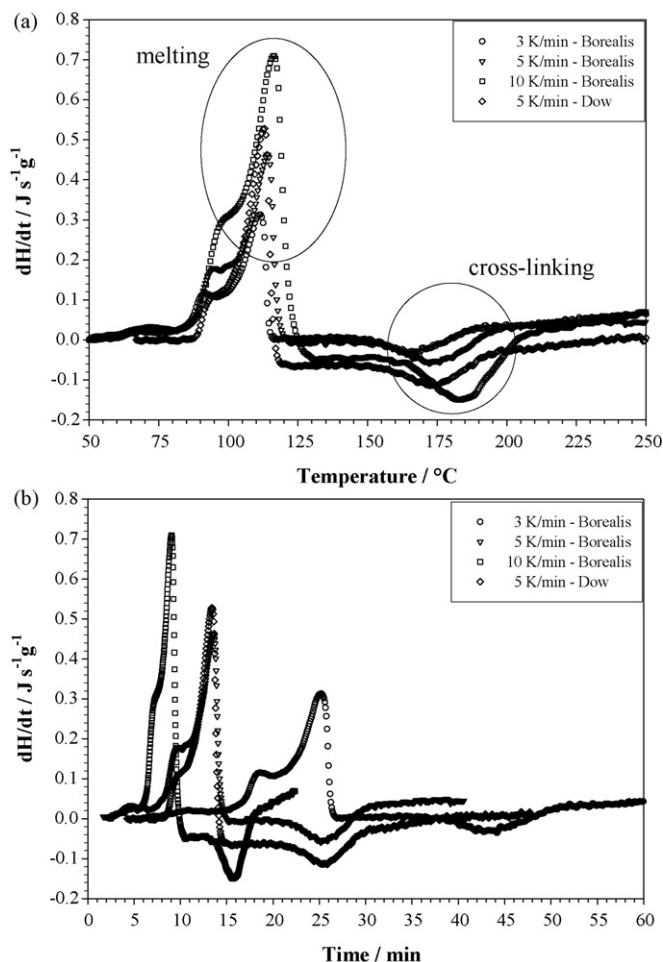


Fig. 7. (a) Rate of heat evolved from the reaction as a function of temperature at chosen heating rates for two preparations of insulation material. (b) Rate of heat evolved from the reaction as a function of time at chosen heating rates for two preparations of insulation material.

tube is fully isolated and there is no possibility for relevant temperature measurement until the cable exits that part. On the other hand the water cooled part of the tube is 'open' so the temperature was measured at the visible part of the tube along the tube wall. Also, after the cable left the tube, the temperature was measured along the cable surface until the end of the process. Temperature was measured with an infrared Raytek sensor with the resolution of $0.1\,°C$ and the accuracy of $\pm 1\,°C$.

### 2.3. Experimental results

#### 2.3.1. DSC analysis

The dynamic DSC analysis was performed at three heating rates: 3, 5, $10\,°C\,min^{-1}$. The sample was heated from the ambient temperature to $250\,°C$. Fig. 7a and b show heat flux ($dH/dt$) as a function of temperature and time at the chosen heating rates. The experiment done at $5\,°C\,min^{-1}$ proves that the two preparations of XLPE 4201 (from Borealis and Dow chemicals) are equal, what is shown in Table 1.

The experimental DSC thermograms are divided in two parts, Fig. 7a: (1) melting of the insulation material between 90 and $120\,°C$ which is an endothermic reaction and (2) cross-linking reaction between 160 and $220\,°C$ which is an exothermic reaction.

#### 2.3.2. Production line temperature measurements

Table 2 presents the measured temperatures of tube wall in the water cooled part of the process (part 3 in Fig. 5), and Table 3

shows the cooling in the final part of the process (part 4 in Fig. 5), where the cable is cooled by the surrounding air.

As shown in Table 2, the position zero meters represents the link point between nitrogen and water (both on pressure of 10 bar), and the measured temperature at this point is in fact a nitrogen temperature. Length of the water cooled part of the tube is 80 m and it finishes with a water seal (Fig. 3) where the cable is passed out the tube. Water passes through the tube in counter current flow against the cable, and the measured flow is around $3\,m^3\,h^{-1}$.

In the last air cooling part of the process, as shown in Table 3, the cable surface is heated up in the first 15 m and after that is

Table 1
Estimated kinetic parameters and the reaction heat at different heating rates for XLPE 4201

| Heating rate ($°C\,min^{-1}$) | $\Delta H_m$ ($J\,g^{-1}$) | $\Delta H_r$ ($J\,g^{-1}$) | $A_r$ ($s^{-1}$) | $E_a$ ($kJ\,mol^{-1}$) | $m$ | $n$ | RMSD ($\times 10^{-3}$) |
|---|---|---|---|---|---|---|---|
| 3 (Borealis) | 75.3672 | −31.8947 | 3833.61 | 48.17 | 0.711 | 1.289 | 2.6283 |
| 5 (Borealis) | 76.1821 | −27.9738 | 4032.07 | 45.96 | 0.711 | 1.289 | 1.5175 |
| 5 (Dow Chemicals) | 73.2052 | −27.5286 | 4053.06 | 45.86 | 0.710 | 1.290 | 2.2738 |
| 10 (Borealis) | 74.8362 | −28.6915 | 4055.12 | 45.84 | 0.710 | 1.290 | 1.5332 |

Table 2
Tube wall temperature along the water cooled part of the process

| Position (m) | Temperature (°C) |
| --- | --- |
| 0 | 176.6 |
| 2 | 112.2 |
| 4 | 83.5 |
| 5.5 | 54.8 |
| 6.5 | 49.1 |
| 9 | 42.6 |
| 11.5 | 39.3 |
| 12.5 | 37.9 |
| 18 | 35.0 |
| 80 | 34.1 |

Table 3
Cable surface temperature during 'free' cooling of the cable in the surrounding air

| Position (m) | Temperature (°C) |
| --- | --- |
| 0 | 34.9 |
| 5 | 47.8 |
| 10 | 50.7 |
| 15 | 53.8 |
| 90 | 49.5 |
| 96 | 43.1 |
| 103 | 42.6 |
| 115 | 40.2 |

cooled to the ambient temperature. This is because of a temperature gradient between the hot core and the cooled surface of the insulation, due to low thermal conductivity of the polymer.

The presented experiments are just a part of the tests performed during this research. A complete experimental set-up requires a study of the used material (insulation and conductor) properties, a detailed scanning of the production process (extruder capacity, etc.), and finally a strict quality control according to the applied standard (IEC 60 502-2). Conducted experiments (DSC—kinetics and process temperatures) were required for a validation of the mathematical model which will be presented in the next section of the paper.

## 3. Mathematical model of the process

Main purpose of this work is a development of a mathematical model of the continuous cross-linking process which will be evaluated by the process simulation.

The presented mathematical model contains main parts of the process described in the experimental: (1) reaction and heating of the cable, (2) cable water cooling, and (3) cable air cooling. In all cases the mathematical model is represented with a set of partial differential equations (PDE) and solved numerically by method of lines for chosen boundary conditions [18,19].

### 3.1. Modeling of the heated part of the tube

Vulcanization tube with moving cable in it can be considered as a tubular reactor where the 'reaction mixture' is a cable itself and for which following assumptions stand [20]:

- Ideal 'plug' cable flow.
- Cross-linking reaction occurred inside the insulation coated over the conductor (cable core).
- Degree of cross-linking through the insulation as well as the temperature inside the cable is a function of both an axial and a radial coordinate.
- The heat is transferred from the tube inner wall heated by external spiral heaters at 350–400 °C to the cable surface. The cable enters the tube with a uniform temperature of 130 °C throughout the core and polymer layer (initial condition). The heat is transferred partially by radiation but also by convection between the heated nitrogen inside the tube and the cable surface.
- Laminar flow of nitrogen around the cable surface is assumed.
- Only radial heat conduction through the cable is assumed.
- Convection and radiation heat transfer are joined in one term $(h + h_r)$ and applied in Eq. (15).
- Thermodynamic parameters $(\rho, \lambda, c_p)$ are assumed constant within the experimental temperature range.
- Due to the stationary process nitrogen temperature in the tube is constant and equal to the tube wall temperature (350–400 °C).

Based on above assumptions mathematical model for this part of the process is given by a set of PDEs:

1. Material balance for the polymer part (insulation):

$$u\rho_p \frac{\partial P}{\partial z} - r_p = 0 \tag{4}$$

2. Kinetic model for the cross-linking reaction occurred in the polymer:

$$r_p = A_r \exp\left(-\frac{E_a}{R_g T}\right) P^n (1 - P)^m \tag{5}$$

3. Heat balance for the cable core (conductor):

$$u\rho_j c_{pj} \frac{\partial T_j}{\partial z} - \lambda_j \left[ \frac{\partial^2 T_j}{\partial r^2} + \frac{1}{r} \frac{\partial T_j}{\partial r} \right] = 0 \tag{6}$$

4. Heat balance for the polymer (insulation):

$$u\rho_p c_{pp} \frac{\partial T_p}{\partial z} - \lambda_p \left[ \frac{\partial^2 T_p}{\partial r^2} + \frac{1}{r} \frac{\partial T_p}{\partial r} \right] + \Delta H_r r_p = 0 \tag{7}$$

5a. Boundary condition at the cable's entrance in the tube, position $z = 0$:

$$P(0, r - d) = 0 \tag{8}$$

$$T_j(0, d) = T_j^0 \tag{9}$$

$$T_p(0, R - d) = T_p^0 \tag{10}$$

5b. Boundary conditions along the radial position:

- $r = R$, cable surface, for all $z$:

$$h(T_{z,R} - T_N) + q_{rad} = -\lambda_p \frac{\partial T}{\partial r} \qquad (11)$$

- $r = d$, insulation–conductor interface, for all $z$:

$$\lambda_p \frac{\partial T_p}{\partial r} = \lambda_j \frac{\partial T_j}{\partial r} \qquad (12)$$

- $r = 0$, cable center:

$$\frac{\partial T_j}{\partial r} = 0 \qquad (13)$$

6. Radiation heat transfer:

$$q_{rad} = \frac{\sigma(T_1^2 + T_2^2)(T_1 + T_2)}{(1/\varepsilon_1) + ((A_1/A_2)((1/\varepsilon_2) - 1))} \qquad (14)$$

Overall heat transfer from the tube wall to the cable surface is assumed to be a joined radiation and convection mechanism. Based on this assumption, Eq. (11) becomes,

$$\frac{\partial T}{\partial r} = \frac{h + h_r}{\lambda_p}(T_{z,R} - T_N) \qquad (15)$$

The main problem during the calculation is instability due to a significant difference between the conductor and the insulation heat conductivity (see Table 6). It results with a steep temperature gradient between the most inner layer of insulation and the core surface. To bypass this problem the lower value of aluminum (Al) thermal conductivity was chosen ($40 \, \text{W m}^{-1} \, \text{K}^{-1}$), and with this assumption the temperature of the cable core is almost constant across its diameter because of a rapid heat transfer through the conductor.

Heat balance for the conductor (Eq. (6)) can be simplified and replaced with a boundary condition between core surface and the most inner insulation layer. So, this equation is

$$\lambda_p \frac{\partial T}{\partial r} = -h_u(T_{i,NB} - T_{i,j}) \qquad (16)$$

where $(T_{i,NB} - T_{i,j})$ is a temperature gradient between the most inner insulation layer and the core temperature, and $h_u$ is a resistant coefficient in a layer between the core and the insulation.

After the heated part of the tube there is a transition part between heating and cooling with water in the unisolated part of the tube which is filled with nitrogen under pressure, but not heated. There are no external heaters in this part of the tube. The cable starts to cool down and it is assumed in this work that no reaction occurs any more. Based on this, heat balances for conductor and insulation are given by

- Conductor:

$$u\rho_j c_{pj} \frac{\partial T_j}{\partial z} - \lambda_j \left[ \frac{\partial^2 T_j}{\partial r^2} + \frac{1}{r}\frac{\partial T_j}{\partial r} \right] = 0$$

- Insulation:

$$u\rho_p c_{pp} \frac{\partial T_p}{\partial z} - \lambda_p \left[ \frac{\partial^2 T_p}{\partial r^2} + \frac{1}{r}\frac{\partial T_p}{\partial r} \right] = 0 \qquad (17)$$

Beside the previously mentioned assumptions about condition in the tube, in this transition part some other also stand:

- Nitrogen is static in the tube, so it predicts stationary conduction through the nitrogen in radial direction from the cable surface to the tube inner wall given by

$$\frac{\partial^2 T_N}{\partial r^2} + \frac{1}{r}\frac{\partial T_N}{\partial r} = 0 \qquad (18)$$

- Also, the tube is cooled by free convection with the surrounding air. The boundary condition at the tube wall is

$$\frac{\partial T_N}{\partial r} = -\frac{h_{air}}{\lambda_N}(T_N - T_{air}) \qquad (19)$$

### 3.2. Modeling of the water cooled part of the tube

Temperature profile exists at the cable exit point (end of the heating zone) with a maximum temperature on the cable surface at around 170 °C. The temperatures should be equalized in the cable radial direction until the end of the process. The cooling is designed in two parts: (a) in the water cooled part of the tube and (b) in the surrounding air after the cable exits the tube. At the end of the water cooled part of the process the temperature across the cable should decrease to around 90 °C. If the cable leaves the tube with a higher temperature (>90 °C) a mechanical damage to the insulation can occur when the cable enters the water seal and collides with the other steel made elements of the production line.

The cooling water flows counter current inside the tube, and from the calculated $Re$ numbers it can be assumed a turbulent flow regime. Having this in mind the main assumption is that the temperature of the cold water in the tube is constant in radial direction, and it changes only in the axial direction. The other assumptions are:

- Initial temperature of the cooling water is known (20–25 °C).
- Cross-linking reaction is finished in the previous part of the process.
- Cable surface is cooled by force convection due to the turbulent water flow.
- Tube wall is cooled in the surrounding air by free convection.
- Water temperature at the cable entrance in the water cooled part of the tube must be known (it is in fact the water exit temperature) as a initial condition for the calculation.

The mathematical model for this part of the process contains previous and some new equations:

1. Heat balance for the cable core (conductor):

$$u\rho_j c_{pj} \frac{\partial T_j}{\partial z} - \lambda_j \left[ \frac{\partial^2 T_j}{\partial r^2} + \frac{1}{r}\frac{\partial T_j}{\partial r} \right] = 0$$

2. Heat balance for the polymer (insulation):

$$u\rho_p c_{pp} \frac{\partial T_p}{\partial z} - \lambda_p \left[ \frac{\partial^2 T_p}{\partial r^2} + \frac{1}{r} \frac{\partial T_p}{\partial r} \right] = 0$$

3. Boundary condition for the cable surface–water interface:

$$\frac{\partial T_p}{\partial r} = -\frac{h_{H_2O}}{\lambda_p}(T_p - T_{H_2O}) \tag{20}$$

4. Heat balance for water flowing in the tube:

$$-u_{H_2O}\rho_{H_2O}c_{pH_2O} \frac{\partial T_{H_2O}}{\partial z} + \frac{h_{H_2O}}{\lambda_p}(T_p - T_{H_2O})$$
$$+ \frac{h_{air}}{\lambda_{H_2O}}(T_{H_2O} - T_{air}) = 0 \tag{21}$$

5. Boundary condition for the tube wall–air interface:

$$\frac{\partial T_w}{\partial r} = -\frac{h_{air}}{\lambda_w}(T_w - T_{air}) \tag{22}$$

### 3.3. Modeling of the air cooled part of the production line

In the last part of the process the cable is air cooled until the end of the line when the product is wheeled up. The cable exits the tube at the water seal (Fig. 3) and in the last hundred meters the temperatures should equalize to the ambient temperature in the radial direction of the cable. There should not be any temperature gradients inside the cable at the end of the process.

The cable can be considered as a heat exchanger with radial heat conduction across the cable (radial direction) and free convection from the cable surface to the surrounding air. The mathematical model will be also a set of partial differential equations with added boundary conditions of heat transfer from the cable surface to the air.

Additional assumptions in this part of the process are:

- Air temperature around the cable is known and it is the same as the ambient temperature.
- Heat is transferred by free convection from the cable surface to the surrounding air.
- Initial temperature distribution in the cable radial direction is known from the end of a previous part of the process (water cooling).

The mathematical model for this final part of the process is given by

1. Heat balance for the cable core (conductor):

$$u\rho_j c_{pj} \frac{\partial T_j}{\partial z} - \lambda_j \left[ \frac{\partial^2 T_j}{\partial r^2} + \frac{1}{r} \frac{\partial T_j}{\partial r} \right] = 0$$

2. Heat balance for the polymer (insulation):

$$u\rho_p c_{pp} \frac{\partial T_p}{\partial z} - \lambda_p \left[ \frac{\partial^2 T_p}{\partial r^2} + \frac{1}{r} \frac{\partial T_p}{\partial r} \right] = 0$$

3. According to the discussion above there is only one new equation which is not previously written for this part of the process and it is boundary condition for the cable surface:

$$\frac{\partial T_p}{\partial r} = -\frac{h_{air}}{\lambda_p}(T_p - T_{air}) \tag{23}$$

## 4. Results and discussion

As a part of the mathematical model, kinetic constants as well as heat transfer coefficients were evaluated. Finally, the main result of this research will be presented in the form of process simulations based on the proposed mathematical model which implement both calculated kinetic parameters as well as the process parameters used during the cable manufacturing.

### 4.1. Cross-linking reaction kinetics

It is usual to use a simple $n$th order kinetic (Eq. (2)) to describe cross-linking reaction governed by the peroxide decomposition as the rate limiting reaction. But, as Fig. 8 shows this model cannot describe an incubation period at the beginning of the reaction during the peroxide decomposition (first 4 min).

In this work a modified kinetic equation was used based on the well-known equation applied for curing system for unsaturated polyester and epoxy resins. For processing of dynamic DSC experiment scans an extended version of the equation is used [11]:

$$r_A = A_r \exp\left(-\frac{E_a}{R_g T}\right) P^n (1 - P)^m \tag{24}$$

with four parameters to estimate $A_r$, $E_a$, and exponents $n$, $m$.
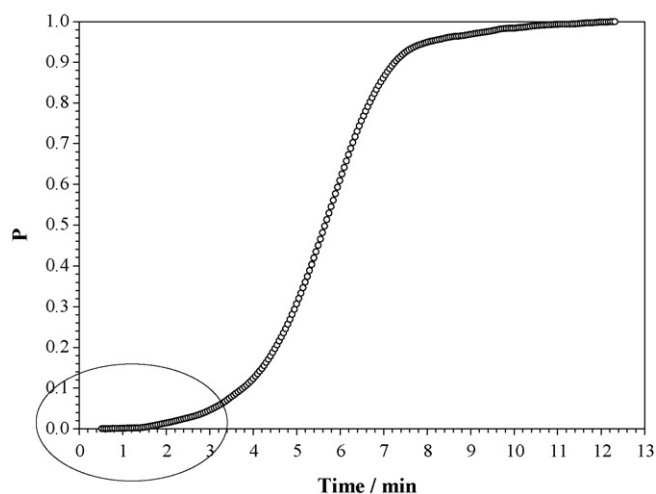


Fig. 8. Theoretical degree of cross-linking as a function of time at the heating rate 5 K min$^{-1}$.

From experimental DSC scans ($dH/dt = f(t, T)$, Fig. 7b, reaction part) it is necessary to evaluate the rate of reaction ($r_A$) and the theoretical degree of cross-linking ($P$) from the next two equations:

$$r_A = \frac{1}{\Delta H_r} \left( \frac{dH}{dt} \right)_t \tag{25}$$

and

$$P = \frac{1}{\Delta H_r} \int_0^t \left( \frac{dH}{dt} \right)_t dt \tag{26}$$

$\Delta H_r$ is a heat of reaction calculated as an area under the peak shown in Fig. 7b (the reaction part).

The Nelder–Mead (modified Simplex) method was used for model parameters estimation together with a root mean square of the normalized variable as error criteria [21]:

$$RMSD = \sqrt{\frac{1}{N} \sum_{i=1}^{N} (\bar{y}_{i_{exp.}} - \bar{y}_{i_{theor.}})^2} \tag{27}$$

The estimated values for the kinetic parameters and the reaction heat at a different heating rate are presented in Table 1.

Given $\Delta H_r$ values show that the cross-linking reaction is faintly exothermic. In the whole complex reaction mechanism only the peroxides decomposition results with some energy dissipation. As we expected kinetic parameters are independent of heating rate. Also, as shown in the results (Table 1) at heating rate 5 K min⁻¹ identical kinetic properties of XLPE 4201 from both material suppliers (Dow Chemicals, and Borealis) were confirmed.

### 4.2. Estimation of heat transfer coefficients

The heat transfer coefficients $h_{H_2O}$ (Eq. (20)), $h_{air}$ (Eq. (23)) are calculated from well known empirical correlations [22].

#### 4.2.1. Force convection cable–water (water cooled part of the tube)

For the turbulent water flow following correlation stands:

$$Nu = 0.023\, Re^{0.8}\, Pr^n, \qquad n = 0.4\text{—heating},$$
$$n = 0.3\text{—cooling} \tag{28}$$

Two types of medium voltage cables were used, so in the following tables they will be mark with indices 1 and 2. The dimensionless numbers must be calculated from:

$$Nu = \frac{hd}{\lambda}, \quad Re = \frac{\rho u d}{\mu}, \quad Pr = \frac{c_p \mu}{\lambda} \tag{29}$$

$$h = \frac{Nu\, \lambda}{d} \tag{30}$$

Estimated values for the heat transfer coefficient between the cable and the turbulent water flow are presented in Table 4. Due to the water flow in the tube, the flow rate ($u$) is calculated as a sum of the water flow rate and the cable speed in the tube.

Table 4
Heat transfer coefficients according to Eqs. (29) and (30)

| Cable | $d$ (m) | $u$ (m s⁻¹) | $Re$ | $Nu$ | $h$ (W m⁻² K⁻¹) |
|---|---|---|---|---|---|
| Force convection cable–water | | | | | |
| 1 | 0.0272 | 0.272 | 44,063 | 161.2 | 1490.2 |
| 2 | 0.0288 | 0.248 | 39,292 | 147.1 | 1390.4 |
| Force convection inner tube wall–water | | | | | |
| 1 | 0.0272 | 0.114 | 18,484 | 80.4 | 743.7 |
| 2 | 0.0288 | 0.116 | 18,314 | 79.9 | 754.8 |

#### 4.2.2. Force convection, the inner tube wall–water

The same as in the previous section $u$, $Re$, $Nu$ and $h$ are calculated from Eqs. (29) and (30), Table 4.

The calculated heat coefficients are lower than in the case of the force convection cable–water due to the lover water flow rate, $u_{H_2O}$.

#### 4.2.3. Free convection tube wall–surrounding air

For the free convection the following correlation stands:

$$Nu = \frac{hd}{\lambda_{air}} = C(Gr_{air}\, Pr_{air})^a \tag{31}$$

The parameters $C$ and $a$ are function of the air flow (laminar or turbulent) and should be taken from the literature for the given multiplier ($Gr \times Pr$). The calculate heat transfer coefficients for different estimated temperatures at the tube wall ($T_{air}$) ranges from 4.6 to 8.8 W m⁻² K⁻¹. During the calculation mean value of $h$ was used.

#### 4.2.4. Overall heat transfer through the tube wall, $U$

The overall heat transfer coefficient ($U$) presents heat transfer resistance through the tube wall from one medium to another (from water to air). In case of the vulcanization tube, $U$ is a cumulative resistance of the heat transfer from cold water to tube inner wall, the conduction through the thick tube wall, and the free convection from outer tube wall to the surrounding air.

It is usual to calculate overall heat transfer for the inside (index 'i') and outside (index 'o') area of the tube. Literature chosen correlations are given by [22]

$$U_i = \frac{1}{(1/h_i A_i) + (A_i\, \ln(r_o/r_i)/2\pi\lambda L) + (A_i/A_o)(1/h_o)} \tag{32}$$

$$U_o = \frac{1}{(A_o/A_i)(1/h_i) + (A_o\, \ln(r_o/r_i)/2\pi\lambda L) + 1/h_o} \tag{33}$$

Overall heat transfer coefficients ($U$) were calculated from Eqs. (32) and (33). Their values are: $U_i = 7.8$ W m⁻² K⁻¹ and $U_o = 6.5$ W m⁻² K⁻¹.

#### 4.2.5. Free convection cable surface–surrounding air

The same correlation stands for the cable–air free convection as for the tube wall–air:

$$Nu = \frac{hd}{\lambda_{air}} = C(Gr_{air}\, Pr_{air})^a$$

Table 5
Process parameters for the cable production line

| Cross-section of conductor (mm$^2$) | $r$(cable) (mm) | $r$(core) (mm) | Line speed (m min$^{-1}$) | $T_1$–$T_3$ (°C) | $T_4$–$T_6$ (°C) |
|---|---|---|---|---|---|
| 150 | 13.6 | 7.05 | 9.5 | 400 | 350 |
| 185 | 14.4 | 7.85 | 8 | 400 | 350 |

It is usual to use the simplified correlation for the cylindrical geometry:

$$h = 1.32 \left( \frac{\Delta T}{d} \right)^{1/4} \tag{34}$$

Same as in case of tube wall–air convection values for $h$ are calculated as function of cable position and measured cable surface temperature (see Table 3, experimental). Also, mean values of calculated $h$ were used, they were between 6.43 and 8.34 W m$^{-2}$ K$^{-1}$.

### 4.3. Simulation of the process

On the basis of proposed mathematical model, simulations of the process were conducted. All simulations were performed with the process parameters used during the medium voltage (MV) cable production. The process parameters and physical constants used in the calculation are presented in Tables 5 and 6. In this part of the paper mainly results for the 185 mm$^2$ MV cable will be presented due to the similarity in simulation results for both cables (150 and 185 mm$^2$).

Temperature of the insulation and the conductor are assumed equal at the beginning of the line and they were 130 °C. Also, the measured water flow was 3 m$^3$ h$^{-1}$.

It is important to mention that the correlation for physical constants as a function of temperature and pressure during the process is added to the mathematical model. This is most important for the water cooled part of the process where the water is under pressure of 10 bar. Water temperature also varies along the tube.

### 4.3.1. Simulation of the heated (reaction) part of the tube

The govern process parameter which is involved in the cross-linking of insulation is line speed. The lower line speed gives a higher residence time of the cable in the tube and as the result a higher DOC across the polymer layer.

Fig. 9 represents values of DOC along the first 36 m of the production line at four different positions in the radial direction of cable. Position $x = 0$, represent dimensionless position in the

Table 6
Physical properties for the used materials at 100 °C

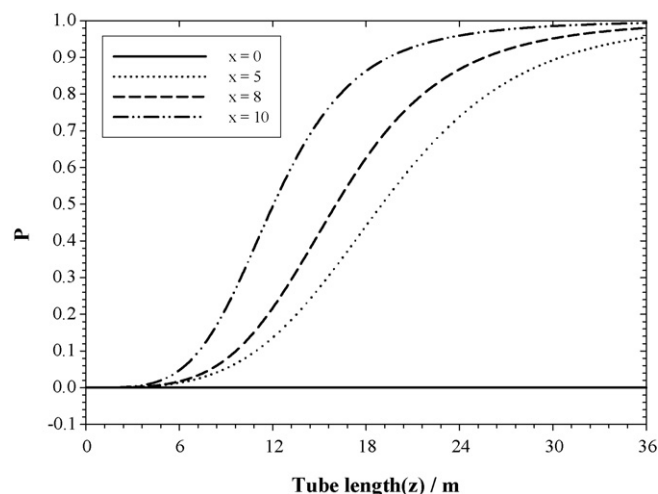| Material | $\rho$ (kg m$^{-3}$) | $c_p$ (J kg$^{-1}$ K$^{-1}$) | $\lambda$ (W m$^{-1}$ K$^{-1}$) |
|---|---|---|---|
| Conductor, Al | 2707 | 896 | 206 |
| Insulation, XLPE 4201 | 922 | 2700 | 0.335 |
| Nitrogen, N$_2$ | 8.53 | 1045 | 0.03335 |
| Water, H$_2$O | 963 | 4200 | 0.665 |



Fig. 9. Calculated DOC profiles along the vulcanization tube ($z$) for different radial positions ($x$).

cable centre, $x = 5$ is the first layer of insulation on the conductor, $x = 8$ is a position of the middle layer of insulation and $x = 10$ is the last layer of the insulation, in fact, the cable surface.

As shown in Table 5 the nitrogen temperature in the first 18 m of the tube is 400 °C. DOC reaches 0.9 on the cable surface, but significantly less through the inner insulation layers. In the second part of the tube (from 18 to 36 m) at the nitrogen temperature of 350 °C, DOC rises to the highest vale at the end (36 m), and it ranges from 0.95 to 0.99 across the insulation radial position.

Fig. 10 represents DOC as a function of the cable radial position for a given position in the tube ($z$). The figure is sep-
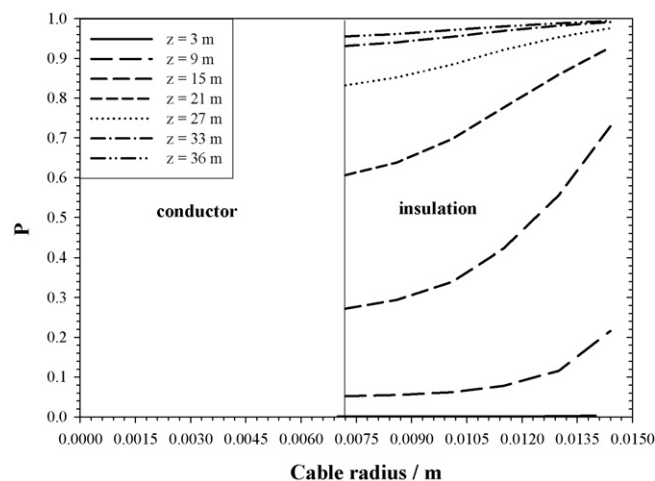


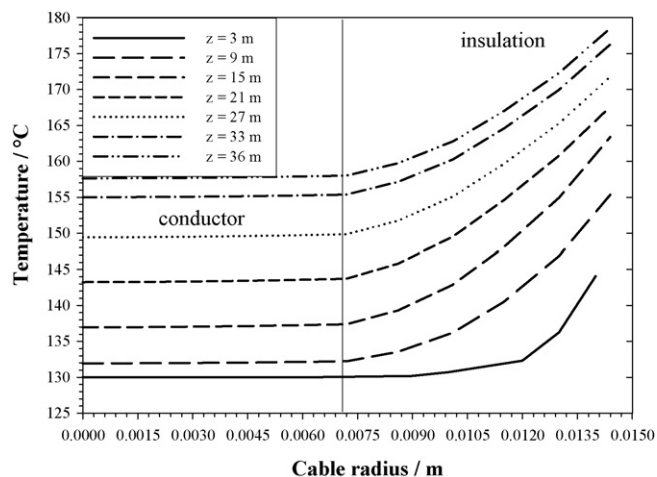Fig. 10. Calculated radial DOC profiles through the cable ($r$) at different position in tube ($z$).

Fig. 11. Calculated radial temperature profiles through the cable ($r$) at different position in the tube ($z$).



Fig. 12. Calculated radial temperature profiles through the cable at different positions in the water part of the tube.

arated in two parts: (a) conductor part (no chemical reaction) and (b) insulation part. Similarly to the previous Fig. 9, DOC rises along the tube and across the insulation as well. Due to the low thermal conductivity of the insulation the heat is slowly transferred through the insulation. At the beginning of the tube, after 3 m, DOC is less than 0.1 with a slight conversion near the conductor surface. As the process continues (higher residence time), DOC arises along the tube length and also becomes even across the insulation radius. At the end of this part of the process after 36 m, DOC should be completely equalized across the insulation. In this case DOC ranges from 0.91 at the core surface to the 0.99 at the cable surface which is satisfying.

The best view for temperature changes during the process is to represent the temperature as a function of cable radius for any given position in the tube (or cable). In the following sections the simulations will be presented for the cable temperatures in the heated part of the tube and also for the cooling in the water cooled part and finally the air cooling.

Fig. 11 shows temperature radial profiles inside the cable in the first 36 m of the process. The graph is divided in two parts, the conductor and the insulation.

Temperature rises from the cable center to the surface. Hot nitrogen heats the cable surface by radiation and convection, and the heat is transferred through the cable by conduction. Due to the high thermal conductivity of aluminum the temperature is nearly constant inside the core which is confirmed by the mathematical model. At the end of this part of the process, after 36 m, the temperature gradient between the core and the cable surface ranges between 155 and 175 °C, and should be equalized in the cooling part until the end of the process.

### 4.3.2. Simulation of the water cooled part of the tube

As a main assumption of the mathematical model, cross-linking reaction finishes in the first 36 m of the process. So, in the following water cooled and finally air cooled part of the process only simulations for the temperature changes during the process will be presented.
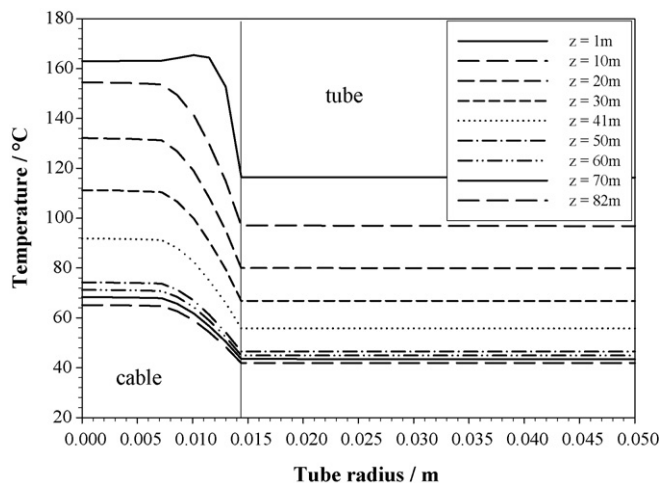
Fig. 12 shows temperature profiles inside the water cooled part of the tube. After the first, heated part of the tube, the tube diameter is reduced from 150 to 100 mm.

In the next 82 m ($z$, Fig. 12) the cable is cooled down with cold water (temperature around 20 °C) which flows inside the tube in a counter current flow regime. The water in the tube is also under pressure of 10 bar. Fig. 12 shows temperature profiles in the radial direction of the cable and water. The cable–water interface is marked with a straight line in Fig. 12, with this in mind the graph is separated in two parts:

(1) The cable cooling (core and insulation) with a temperature gradient still present after 82 m of 40–60 °C.
(2) The temperature profile of water inside the tube. The water temperature is constant in the radial direction because of a turbulent water flow in the tube.

### 4.3.3. Simulation of the air cooled part of the process

At the end of the process cable is cooled in the surrounding air. In the next 115 m the cable temperature in the entire profile should decrease to around 40 °C.

It is seen from Fig. 13 that the majority of the cooling occurs in the first 5 m of the cable presence in the surrounding air. It is reasonable because of a high temperature gradient between the cable and the air. As mentioned earlier and shown in the experimental part, the temperature on the cable surface ($r = 0.014$ m) rises in the first 10 m. This can be explained by a delayed heat transfer from the cable core to the surface. The end temperature after 114 m is even in the cable and it is around 33 °C which is similar to the experimental values (Table 3, 40 °C).

Finally, joined picture form all tree main parts can be presented. Fig. 14 shows temperature profiles in the radial direction as function of the complete process length (240 m).

At the first 36 m in the heated part of the tube the temperature rises across the cable diameter with the maximum at the cable surface ($x = 10$). In the next 6 m the tube is filled with nitrogen but not heated, this part can be described as a transition section
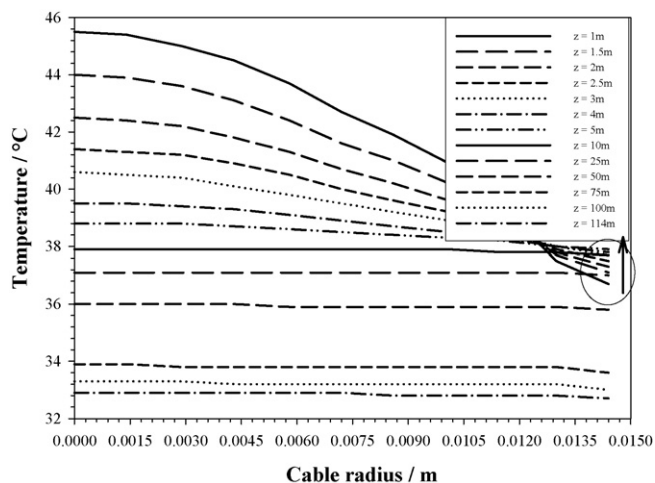
Fig. 13. Calculated radial temperature profiles through the cable at different position in a free air cooling part of the process.

between the cable heating and cooling. After that the cable enters the water cooled part of the tube. Due to the heat transferred from the core, the temperature increases in the first 10 m at the cable surface, but after that it starts to cool down. At the end of the water cooling after 125 m the cable is cooled down to the temperature of 35 °C on the surface and to 50 °C in the cable center.

At this point the temperature gradients are still present across the cable diameter. The last part of the process is the cable cooling in the surrounding air after the water cooled part. As shown in the experimental part in the first 10–15 m the temperature of cable surface rises. Finally, after 240 m of the process, the temperature of the cable is decreased to the ambient temperature at around 30 °C and it must be equal across the whole radius.

From the present simulations (Figs. 9–14) it is obvious that the mathematical model is a good description of the industrial process of the power cable processing. The simulations also show that the used process parameters values (line speed, tem-
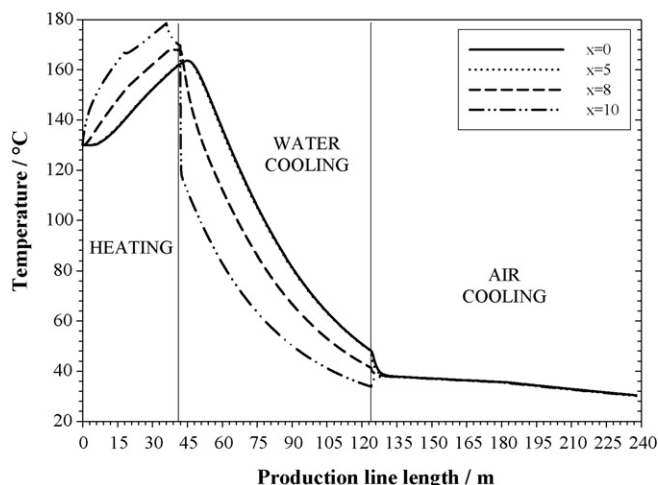
perature, cooling regime, etc.) and thermodynamic parameters (for cable materials and heating (cooling) media) are the right ones.

## 5. Conclusions

Cross-linking reaction kinetics was estimated from the independent (DSC) measurements. The reaction enthalpy and kinetic parameters were calculated. Their values are: $\Delta H_r = 30\,\mathrm{J\,g^{-1}}$, $E_a = 46\,\mathrm{kJ\,mol^{-1}}$, $A_r = 4000\,\mathrm{s^{-1}}$, $m = 0.71$ and $n = 1.23$. The reaction enthalpy is rather small. This means that the reaction part can be neglected in comparison with other terms in the mathematical model.

The proposed mathematical model describes process in all of their tree main parts: (1) reaction tube, (2) water cooling and (3) air cooling. The mathematical model is defined by a set of partial differential equations (PDE) and it is solved numerically for the given boundary conditions. The used numerical method was the method of lines. Based on the mathematical model and real process parameters the process simulation was executed. The presented simulations confirm that the empirically chosen process parameters which have been used over a decade for production of medium voltage cables on this plant (line speed $8\,\mathrm{m\,min^{-1}}$, nitrogen temperature in the tube, $T_1$–$T_3 = 400$ °C, $T_4$–$T_6 = 350$ °C, water flow $3\,\mathrm{m^3\,h^{-1}}$) are a good manufacturer's selection. Also, the chosen literature thermo-dynamical properties ($\rho$, $c_p$, $\lambda$) for the used materials (aluminium, XLPE, nitrogen, water, air) can be used in the wide area of process temperatures. On the basis of the presented simulations optimal process parameters such as process temperatures, speed capacities and cable cooling properties for the CV line could be predicted and evaluated for a wide range of MV/HV cables.

The future work will expand the kinetic experiments with some other methods like FT-IR [23], in the purpose of confirming the cross-linking reaction kinetic determined by DSC.

## References

[1] W.C. Endstra, Paper Presented at the DTK'88, 1988.
[2] L.H.U. Andersson, B. Gustafsson, T. Hjertberg, Polymer 45 (2004) 2577–2585.
[3] T. Yamazaki, T. Segutchi, J. Polym. Sci. A: Polym. Chem. 38 (2000) 3092–3999.
[4] M.T. Shaw, S.H. Shaw, IEEE Trans. Electr. Insulation EI-19 (1984) 419–452.
[5] T. Kang, C. Ha, Polym. Test. 19 (2000) 773–783.
[6] S. Camara, B.C. Gilbert, J.R. Meier, M. van Duin, A.C. Whitwood, Polymer 47 (2006) 4683–4693.
[7] D.M. Martins, J.V. Gulmine, L. Akcelrud, R.C. Weiss, T.D.Z. Atvars, Polymer 47 (2006) 7414–7424.
[8] M. Uhniat, S. Kudla, Polym. Degrad. Stabil. 71 (2001) 69–74.
[9] M. Liu, W. Yu, C. Zhou, J. Yin, Polymer 46 (2005) 7605–7611.
[10] A. Smedberg, T. Hjertberg, B. Gustafsson, Polymer 45 (2004) 4867–4875.
[11] S.Y. Pusatcioglu, J.C. Hassler, A.L. Fricke, J. Appl. Polym. Sci. 24 (1979) 937–946.
[12] K. Suzuki, S. Saito, S. Yoshida, IEEE Trans. Electr. Insulation EI-21 (1986) 945–952.
[13] R.L. Boysen, Presented at the Institute of Electrical and Electronics Engineers, 1970, pp. 1–14.

Fig. 14. Calculated temperature profiles along the whole production line ($z$) at different radial positions ($x$).

[14] IEC, CEI, 1994, pp. 1–79.
[15] D.A. Dahills, Heat Transfer and Vulcanisation of Rubber, Elsevier, 1971.
[16] R.W. Fahien, Fundamentals of Transport Phenomena, McGraw-Hill, New York, 1983.
[17] G. Matey, C. Richardson, Wire Ind. (1990) 35–40.
[18] S.J. Farlow, Partial Differential Equations for Scientists and Engineers, John Wiley & Suns, New York, 1982.
[19] W.E. Schiesser, The Numerical Method of Lines: Integration of Partial Differential Equations, Academic Press, San Diego, 1991.
[20] Y.D. Schkalle, Wireworld 1 (1988) 28–33.
[21] D.M. Himmelblau, Process Analysis by Statistical Methods, John Wiley & Sons, New York, 1970.
[22] J.P. Holman, Heat Transfer, McGraw-Hill, Tokyo, 1981.
[23] M. Uhniat, M. Sudol, S. Kudla, Polym. Degrad. Stab. 71 (2001) 75–82.